

See discussions, stats, and author profiles for this publication at: <https://www.researchgate.net/publication/8423769>

# Organic Cross-Linked Electropolymers as Supported Oxidation Catalysts: Poly((tetrakis(9,9'-spirobifluorenyl)porphyrin)manganese) Films

ARTICLE in INORGANIC CHEMISTRY · SEPTEMBER 2004

Impact Factor: 4.76 · DOI: 10.1021/ic049641b · Source: PubMed

CITATIONS

21

READS

33

## 5 AUTHORS, INCLUDING:



Cyril Poriel

Université de Rennes 1

74 PUBLICATIONS 1,008 CITATIONS

SEE PROFILE



Paul Le Maux

Université de Rennes 1

84 PUBLICATIONS 1,423 CITATIONS

SEE PROFILE



Joëlle Rault-Berthelot

Université de Rennes 1

106 PUBLICATIONS 1,711 CITATIONS

SEE PROFILE



Gérard Simonneaux

Université de Rennes 1

184 PUBLICATIONS 2,685 CITATIONS

SEE PROFILE

## Organic Cross-Linked Electropolymers as Supported Oxidation Catalysts: Poly((tetrakis(9,9'-spirobifluorenyl)porphyrin)manganese) Films

Cyril Poriel,<sup>†</sup> Yann Ferrand,<sup>†</sup> Paul Le Maux,<sup>†</sup> Joëlle Rault-Berthelot,<sup>\*,‡</sup> and Gérard Simonneaux<sup>\*,†</sup>*Laboratoire de Chimie Organométallique et Biologique, UMR CNRS 6509, and Laboratoire d'Electrochimie Moléculaire et Macromoléculaire, UMR CNRS 6510, Université de Rennes 1, 35042 Rennes Cedex, France*

Received March 18, 2004

Anodic oxidation of free base and manganese complexes of tetraspirobifluorenylporphyrins leads to the coating of the working electrode by insoluble electroactive poly(9,9'-spirobifluorene-free and manganese porphyrin) films which electrochemical behavior and physicochemical properties are described. After removal from the electrode, the manganese-complexed polymers were evaluated as catalysts for the oxidation of alkenes by iodobenzene diacetate or iodosylbenzene. The results show that the reactions proceeded very efficiently at room temperature with good yields. The electrosynthesized polymer catalysts can be recycled by simple filtration and reused even up to the eighth cycle without loss of activity and selectivity. These results represent an important improvement over those previously described for manganese-porphyrin-catalyzed epoxidation reactions.

## Introduction

The epoxidation of alkenes, which produces valuable intermediates in organic synthesis, is one of the most thoroughly investigated reactions in homogeneous catalysis. For example, the manganese salen complex developed by Jacobsen and co-workers is known as one of the best catalysts for asymmetric epoxidation of conjugated alkenes.<sup>1</sup> Although homogeneous catalytic processes often display high activity and stereoselectivity, in most cases the catalyst–product separation is very difficult and the metal catalysts and ligands can be quite expensive. Supporting transition metal catalytic complexes on organic polymers have an important role in the development of heterogeneous catalysis.<sup>2</sup> Thus, organo-metallic complexes with catalytic activity can be incorporated into polymers in a variety of methods.<sup>3</sup> A preformed polymer is functionalized with a ligand which is used to bind the metal. However, under the conditions needed to catalyze

organic reactions, desorption of the catalytic entity is possible if there is a labile coordination bond. If weakly coordinating solvents, reagents, and products are present, metal leaching may be minimal, but coordinating solvents will accelerate catalyst leaching. Another synthetic approach involves the preparation of a monomer, which contains the ligand metal complex, followed by the polymerization of the monomer to generate the desirable polymer. In this case, several key advantages exist. First, distribution of active sites throughout the polymer is assured at the microstructural level. Second the degree of cross-linking can be systematically varied. Finally, the nature of the polymer matrix can be varied depending on the number of polymerization sites. However, this approach also presents problems. Monomers containing metal complexes may undergo undesirable reactions with radical, basic, or acid initiators which preclude good polymerization behavior. In this study, we take advantage of electropolymerization to prepare organic polymers which can be easily removed from electrodes and used in heterogeneous oxidation catalysis.

Numerous methods for immobilizing metalloporphyrins under insoluble materials have been reported. Initial methods of immobilization have been reviewed previously.<sup>4</sup> They

\* Authors to whom correspondence should be addressed. E-mail: gerard.simonneaux@univ-rennes1.fr (G.S.).

<sup>†</sup> Laboratoire de Chimie Organométallique et Biologique.

<sup>‡</sup> Laboratoire d'Electrochimie Moléculaire et Macromoléculaire.

(1) Jacobsen, E. N.; Zhang, W.; Muci, L. C.; Ecker, J. R.; Deng, L. J. *Am. Chem. Soc.* **1991**, *113*, 7063.

(2) Gladysz, J. A. *Pure Appl. Chem.* **2001**, *73*, 1319–1324.

(3) Pittman, C. U., Jr. In *Comprehensive Organometallic Chemistry*; Wilkinson, Ed.; Pergamon Press: Oxford, U.K., 1982; Vol. 8, pp 553–611.

(4) Lindsay Smith, J. R. In *Metalloporphyrins in Catalytic Oxidation*; Sheldon, R. A., Ed.; Marcel Dekker: New York, 1994; Chapter 11.

frequently involve fixation of metalloporphyrin catalysts on inorganic supports such as silica gel,<sup>5–14</sup> zeolites,<sup>15–17</sup> montmorillonite,<sup>18–22</sup> gold electrodes,<sup>23</sup> rhenium clusters,<sup>24</sup> and solid-state metal phosphonates.<sup>25,26</sup> Manganese porphyrins have been recently immobilized as a monolayer film by a combination of Langmuir–Blodgett and self-assembled monolayer techniques that use zirconium phosphonate linkages.<sup>27</sup> Organic polymers, such as poly(ethylene glycol),<sup>28–30</sup> ion-exchange resins,<sup>31–35</sup> isocyanide polymers,<sup>36</sup> and polypeptides<sup>37–41</sup> have also been used to support metalloporphyrins.

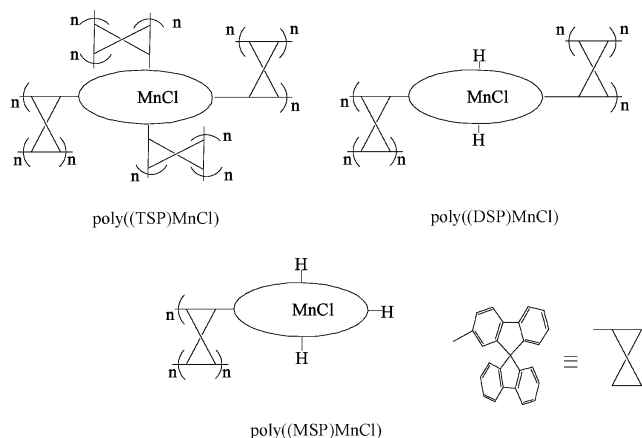
In this case, the polymer is functionalized and the porphyrin is attached through a covalent bond to the material. In contrast, there are very few organic polymers containing metalloporphyrins prepared by chemical polymerization of metalloporphyrin monomers.<sup>42,43</sup>

Since the first report of Macor and Spiro,<sup>44</sup> the immobilization of metalloporphyrins onto electrodes has been carried out mainly by electropolymerization. Conducting metalloporphyrin polymers such as polypyrrole,<sup>45–50</sup> polythiophene,<sup>51</sup> polyaniline,<sup>50</sup> and others<sup>52,53</sup> are attractive as possible materials for this approach.<sup>54,55</sup> However, pyrrole and its derivatives<sup>45,47–49,56–60</sup> are the most frequently used compounds for the formation of conducting polymers, mainly due to the high flexibility in its molecular design and its easy formation from different aqueous and nonaqueous solvents. Functionalization of polypyrrole films by means of metalloporphyrins has been performed by incorporation of the metalloporphyrin complexes into pyrrole films using the ion-exchange properties of the oxidized polymer or by direct electrochemical polymerization of pyrrole-substituted metalloporphyrins. However, in no case were the polymers removed from the electrode to be tested in heterogeneous catalysis, probably due to technical difficulties.

In this report, we describe the development of novel electropolymers for the catalytic oxidation of organic derivatives. The synthesis is based on the electrochemical formation of a poly((spirobifluorenylporphyrin)manganese) film, exhibiting the electrochemical properties of the manganese complex. Surprisingly, even though the oxidation potential needed for polymerization is largely above that of the metal or porphyrin, the metalloporphyrin unit identity is largely maintained. After removal of the electropolymer from the electrode, these insoluble materials have been used for alkene

- (5) Leal, O.; Anderson, D. L.; Bowman, R. G.; Basolo, F.; Burwell, R. L., Jr. *J. Am. Chem. Soc.* **1975**, *97*, 5125–5129.
- (6) Battioni, P.; Lallier, J. P.; Barloy, L.; Mansuy, D. *J. Chem. Soc., Chem. Commun.* **1989**, 1149–1151.
- (7) Nakamura, M.; Tatsumi, T.; Tominaga, H. *Bull. Chem. Soc. Jpn.* **1990**, *63*, 3334–3336.
- (8) Cooke, P. R.; Lindsay Smith, J. R. *Tetrahedron Lett.* **1992**, *33*, 2737–2740.
- (9) Cooke, P. R.; Lindsay Smith, J. R. *J. Chem. Soc., Perkin Trans. 1* **1994**, 1913–1923.
- (10) Gilmartin, C.; Lindsay Smith, J. R. *J. Chem. Soc., Perkin Trans. 2* **1995**, 243–251.
- (11) Hilal, H. S.; Jondi, W.; Khalaf, S.; Keilani, A.; Suleiman, M.; Schreiner, A. F. *J. Mol. Catal., A* **1996**, *113*, 35–44.
- (12) Dore Assis, M. D.; Lindsay Smith, J. R. *J. Chem. Soc., Perkin Trans. 2* **1998**, 2221–2226.
- (13) Evans, S. V.; Lindsay Smith, J. R. *J. Chem. Soc., Perkin Trans. 2* **2001**, 174–180.
- (14) Schiavon, M. A.; Iamamoto, Y.; Nascimento, O. R.; Assis, M. D. *J. Mol. Catal., A* **2001**, *174*, 213–222.
- (15) Battioni, P.; Iwanejko, R.; Mansuy, D.; Młodnicka, T.; Polowicz, J.; Sanchez, F. *J. Mol. Catal., A* **1996**, *109*, 91–98.
- (16) Bedioui, F. *Coord. Chem. Rev.* **1995**, *144*, 39–68.
- (17) Li, Z.; Xia, C. G.; Zhang, X. M. *J. Mol. Catal., A* **2002**, *185*, 47–56.
- (18) Cady, S. S.; Pinnavaia, T. J. *Inorg. Chem.* **1978**, *17*, 1501–1507.
- (19) Kameyama, H.; Suzuki, H.; Amano, A. *Chem. Lett.* **1988**, 1117–1120.
- (20) Barloy, L.; Battioni, P.; Mansuy, D. *J. Chem. Soc., Chem. Commun.* **1990**, 1365–1367.
- (21) Barloy, L.; Lallier, J. P.; Battioni, P.; Mansuy, D.; Piffard, Y.; Tournoux, M.; Valim, J. B.; Jones, W. *New. J. Chem.* **1992**, *16*, 71–80.
- (22) Martinez-Lorente, M. A.; Battioni, P.; Kleemiss, W.; Bartoli, J. F.; Mansuy, D. *J. Mol. Catal., A* **1996**, *113*, 343–353.
- (23) Collman, J. P.; Ennis, M. S.; Offord, D. A.; Chng, L. L.; Griffin, J. H. *Inorg. Chem.* **1996**, *35*, 1751–1752.
- (24) Kim, Y. H.; Choi, S. K.; Park, S. M.; Nam, W.; Kim, S. J. *Inorg. Chem. Commun.* **2002**, *5*, 612–615.
- (25) Deniaud, D.; Schöllorn, B.; Mansuy, D.; Rouxel, J.; Battioni, P.; Bujoli, B. *Chem. Mater.* **1995**, *7*, 995–1000.
- (26) Deniaud, D.; Spyroulias, G. A.; Bartoli, J. F.; Battioni, P.; Mansuy, D.; Pinel, C.; Odobel, F.; Bujoli, B. *New. J. Chem.* **1998**, 901–905.
- (27) Benitez, I. O.; Bujoli, B.; Camus, L. J.; Lee, C. M.; Odobel, F.; Talham, D. R. *J. Am. Chem. Soc.* **2002**, *124*, 4363–4370.
- (28) Zhang, J. L.; Che, C. M. *Org. Lett.* **2002**, *4*, 1911–1914.
- (29) Brulé, E.; de Miguel, Y. R. *Tetrahedron Lett.* **2002**, *43*, 8555–8558.
- (30) Benaglia, M.; Danelli, T.; Pozzi, G. *Org. Biomol. Chem.* **2003**, *1*, 454–456.
- (31) Saito, Y.; Sartouchi, M.; Mifune, M.; Tai, T.; Odo, J.; Tanaka, Y.; Chikuma, M.; Tanaka, H. *Bull. Chem. Soc. Jpn.* **1987**, *60*, 2227–2230.
- (32) Labat, G.; Meunier, B. *J. Org. Chem.* **1989**, *54*, 5008–5011.
- (33) Leanord, D. R.; Lindsay Smith, J. R. *J. Chem. Soc., Perkin Trans. 2* **1990**, 1917–1923.
- (34) Leanord, D. R.; Lindsay Smith, J. R. *J. Chem. Soc., Perkin Trans. 2* **1991**, 25–30.
- (35) Campestrini, S.; Meunier, B. *Inorg. Chem.* **1992**, *31*, 1999–2006.
- (36) van der Made, A. W.; H., S. J. W.; Nolte, R. J. M.; Drenth, W. J. *Chem. Soc., Chem. Commun.* **1983**, 1204–1206.
- (37) Mori, T.; Santa, T.; Hirobe, M. *Tetrahedron Lett.* **1985**, *26*, 5555–5558.
- (38) Higushi, T.; Hirobe, M. *J. Mol. Catal., A* **1996**, *113*, 403–422.
- (39) Geier, G. R., III; Sasaki, T. *Tetrahedron* **1999**, *55*, 1859–1870.
- (40) Geier, G. R., III; Lybrand, T. P.; Sasaki, T. *Tetrahedron* **1999**, 1871–1880.
- (41) Yu, X. Q.; Huang, J. S.; Yu, W. Y.; Che, C. M. *J. Am. Chem. Soc.* **2000**, *122*, 5337–5342.
- (42) Traylor, T. G.; Byun, Y. S.; Traylor, P. S.; Battioni, P.; Mansuy, D. *J. Am. Chem. Soc.* **1991**, *113*, 7821–7823.
- (43) Nestler, O.; Severin, K. *Org. Lett.* **2001**, *3*, 3907–3909.
- (44) Macor, K. A.; Spiro, T. G. *J. Am. Chem. Soc.* **1983**, *105*, 5601–5607.
- (45) Deronzier, A.; Moutet, J. C. *Acc. Chem. Res.* **1989**, *22*, 249–255.
- (46) Deronzier, A.; Moutet, J. C. *Coord. Chem. Rev.* **1996**, *147*, 339–371.
- (47) Cosnier, S.; Gondran, C.; Wessel, R.; Montforts, F. P.; Wedel, M. *J. Electroanal. Chem.* **2000**, *488*, 83–91.
- (48) Cosnier, S.; Gondran, C.; Gorgy, K.; Wessel, R.; Montforts, F. P.; Wedel, M. *Electrochem. Commun.* **2002**, *4*, 426–430.
- (49) Diab, N.; Sculmann, W. *Electrochim. Acta* **2001**, *47*, 265–273.
- (50) Bettelheim, A.; White, B. A.; Raybuck, S. A.; Murray, R. W. *Inorg. Chem.* **1987**, *26*, 1009–1017.
- (51) Maruyama, H.; Segawa, H.; Sotoda, S.; Sato, T.; Kosai, N.; Sagisaka, S.; Shimidzu, T.; Tanaka, K. *Synth. Met.* **1998**, *96*, 141–149.
- (52) Czuchajowski, L.; Bennett, J. E.; Goszczynski, S.; Wheeler, D. E.; Wisor, A. K.; Malinski, T. *J. Am. Chem. Soc.* **1989**, *111*, 607–616.
- (53) Saito, M.; Endo, A.; Shimizu, K.; Satō, G. P. *Electrochim. Acta* **2000**, *45*, 3021–3028.
- (54) Bedioui, F.; Devynck, J.; Bied-Charreton, C. *Acc. Chem. Res.* **1995**, *28*, 30–36.
- (55) Bedioui, F.; Devynck, J.; Bied-Charreton, C. *J. Mol. Catal.* **1996**, *113*, 3–11.
- (56) Bedioui, F.; Merino, A.; Devynck, J.; Mestres, C. E.; Bied-Charreton, C. *J. Electroanal. Chem.* **1988**, *239*, 433–439.
- (57) Moisy, P.; Bedioui, F.; Robin, Y.; Devynck, J. *J. Electroanal. Chem.* **1988**, *250*, 191–199.
- (58) Ramachandralah, G.; Bedioui, F.; Devynck, J.; Serrar, M.; Bied-Charreton, C. *J. Electroanal. Chem.* **1991**, *319*, 395–402.
- (59) Deronzier, A.; Devaux, R.; Limosin, D.; Latour, J. M. *J. Electroanal. Chem.* **1992**, *324*, 325–337.
- (60) Allietta, N.; Pansu, R.; Bied-Charreton, C.; Albin, V.; Bedioui, F.; Devynck, J. *Synth. Met.* **1996**, *81*, 205–210.

epoxidation by iodobenzene diacetate or iodosylbenzene. Three different types of polymers have been synthesized using either a tetraspirobifluorenylporphyrin Mn, (TSP)-MnCl, a dispirobifluorenylporphyrin Mn, (DSP)MnCl or a monospirobifluorenylporphyrin Mn, (MSP)MnCl. Comparison of catalytic activity of these polymers with their homogeneous counterparts in oxidation is also presented.



## Experimental Section

**General Experiments.** All reactions were performed under argon and were magnetically stirred. Solvents were distilled from appropriate drying agent prior to use: Et<sub>2</sub>O and THF from sodium and benzophenone; toluene from sodium; CH<sub>2</sub>Cl<sub>2</sub> from CaH<sub>2</sub>; CHCl<sub>3</sub> from P<sub>2</sub>O<sub>5</sub>. All other solvents were HPLC grade. DMF was purified under azeotropic distillation using a mixture benzene/water. Commercially available reagents were used without further purification unless otherwise stated. All reactions were monitored by TLC with Merck precoated aluminum foil sheets (Silica gel 60 with fluorescent indicator UV<sub>254</sub>). Compounds were visualized with UV light at 254 and 365 nm. Column chromatography was carried out using silica gel from Merck (0.063–0.200 mm). <sup>1</sup>H NMR and <sup>13</sup>C NMR in CDCl<sub>3</sub> and toluene-*d*<sub>8</sub> were recorded using Bruker (Advance 500dpx and 300dpx) spectrometers at 500 and 75 MHz, respectively. The assignments were performed by 2D NMR experiments: COSY (correlation spectroscopy); HMBC (heteronuclear multiple bond correlation); HMQC (heteronuclear multiple quantum coherence). High-resolution mass spectra were recorded on a ZabSpec TOF Micromass spectrometer in the FAB mode or ESI positif mode at the CRMPO.

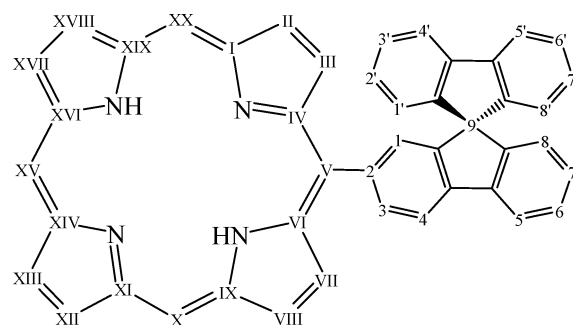
All electrochemical experiments were performed using a Pt disk electrode (diameter 1 mm), the counter electrode was a vitreous carbon rod, and the reference electrode was a silver wire in a 0.1 M AgNO<sub>3</sub> solution in CH<sub>3</sub>CN. Ferrocene was added to the electrolyte solution at the end of a series of experiments. The ferrocene/ferrocenium (Fc/Fc<sup>+</sup>) couple served as internal standard, and all reported potentials were referenced to its reversible formal potential. Activated Al<sub>2</sub>O<sub>3</sub> was added in the electrolytic solution to remove excess moisture. The three-electrode cell was connected to a PAR model 173 potentiostat monitored with a PAR model 175 signal generator and a PAR model 179 signal coulometer. The cyclic voltammetry traces (CVs) were recorded on an XY SEFRAM-type TGM 164.

Dichloromethane with less than 100 ppm of water (reference SDS 02910E21) and tetrabutylammonium hexafluorophosphate from Fluka were used without any purification. Aluminum oxide was obtained from Woelm, activated by heating at 300 °C under vacuum for 12 h and used at once under argon pressure.

Liquid UV–visible spectra were recorded on a UVIKON XL from Biotech. Solid UV–visible spectra were recorded using, either a Guided Wave model 150 spectrophotometer with optical fibers, a concave platinum surface acting as a reflector for the optical beam, or a JASCO-V570 spectrophotometer, the deposit being on an ITO electrode. Scanning electron microscopy was performed on JEOL JSM 301F. Electronic microanalysis was performed on JEOL JSM 6400 using an energy dispersive spectrometry (EDS) detector (Oxford-Link Isis). Infrared spectra were performed with a KBr disk in a IFS 28 Bruker.

All catalytic reactions were controlled on a Varian CP-3380 gas chromatograph equipped with a CP-Chirasil-Dex column. Iodosylbenzene was prepared according to a literature procedure.<sup>61</sup>

**Syntheses.** Synthesis and spectroscopic data of tetrasubstituted (TSP)H<sub>2</sub> and disubstituted (DSP)H<sub>2</sub> free-base porphyrins were reported in previous papers.<sup>62</sup> Labeling for NMR assignments is shown as follows:



**(*meso*-5,10,15,20-Tetrakis(spirobifluoren-2-yl)porphyrinato)-manganese Chloride.** To a solution of (TSP)H<sub>2</sub> (320 μmol) dissolved in 130 mL of distilled and degassed chloroform was added several drops of 2,6-lutidine, anhydrous MnCl<sub>2</sub> finely crushed (4.8 mmol), and dry methanol (10 mL). The mixture was stirred under an argon atmosphere at 50 °C for 10 h until the reaction was completed. The reaction was monitored by UV spectroscopy. The solvent was removed under vacuum, one drop of hydrochloric acid was added, and the crude product was chromatographed on silica gel using first a mixture of pentane/dichloromethane (1/1) to remove unreacted (TSP)H<sub>2</sub> and then dichloromethane/methanol (7/1) to get the manganese complex. The major green band was collected, dried under vacuum, and crystallized in a mixture of dichloromethane/pentane to afford a green powder of (*meso*-tetrakis(5,10,15,20-spirobifluoren-2-yl)porphyrinato)manganese chloride. Yield: 85%. <sup>1</sup>H NMR (CDCl<sub>3</sub>, ppm): –23.3 (H β pyrrole, s br, 8H). UV–vis (CH<sub>2</sub>Cl<sub>2</sub>) [λ<sub>max</sub>/nm (log ε/M<sup>–1</sup> cm<sup>–1</sup>): 228 (5.21), 297 (4.74), 309 (4.79), 336 (4.63), 382 (4.67), 407 (4.67), 481 (5.04), 587 (3.92), 625 (4.11). Mass (ESI, 9/1 CH<sub>2</sub>Cl<sub>2</sub>/MeOH) (*m/z*): calcd for C<sub>120</sub>H<sub>68</sub>N<sub>4</sub>Mn (M – Cl)<sup>+</sup>, 1620.4858; found, 1620.4874. CV in CH<sub>2</sub>Cl<sub>2</sub> + 0.2 M Bu<sub>4</sub>NPF<sub>6</sub> (*E*, V vs Fc/Fc<sup>+</sup>): 0.65, 1.18, 1.33.

**(5,15-Bis(spirobifluoren-2-yl)porphyrinato)manganese Chloride.** This compound was prepared according to the procedure described for *meso*-tetrakis(5,10,15,20(spirobifluoren-2-yl)porphyrinato)manganese chloride. The time reaction was reduced to 4 h. Yield: 72%. <sup>1</sup>H NMR (CDCl<sub>3</sub>, ppm): –24.4 (H β pyrrole, s br, 4H), –22.1 (H β pyrrole, s br, 4H), 47 (H<sub>XX</sub> *meso*, s br, 2H). UV–vis (CH<sub>2</sub>Cl<sub>2</sub>) [λ<sub>max</sub>/nm (log ε/M<sup>–1</sup> cm<sup>–1</sup>): 227 (4.68), 310 (4.16), 372 (4.32), 397 (4.23), 472 (4.64), 572 (3.63), 605 (3.56).

(61) Saltzman, H.; Sharefkin, J. G. *Org. Synth.* **1973**, *5*, 658–659.

(62) Poriel, C.; Ferrand, Y.; Juillard, S.; Le Maux, P.; Simonneaux, G. *Tetrahedron* **2004**, *60*, 145–158.



Mass (ESI: 9/1 CH<sub>2</sub>Cl<sub>2</sub>/MeOH) (*m/z*): calcd for C<sub>70</sub>H<sub>40</sub>N<sub>4</sub>Mn (M – Cl)<sup>+</sup>, 991.2633; found, 991.2624. CV in CH<sub>2</sub>Cl<sub>2</sub> + 0.2 M Bu<sub>4</sub>NPF<sub>6</sub> (*E*, V vs Fc/Fc<sup>+</sup>): 0.69, 1.33.

**5-(Spirobifluoren-2-yl)porphyrin.** Pyrrole-2-carbaldehyde (4 mmol), dipyrromethane (2.06 mmol), and 9,9'-spirobifluorene-2-carbaldehyde (2.06 mmol) were allowed to react at room temperature in dry and degassed dichloromethane (1 L) under an argon atmosphere and protected from light with acid catalysis (CF<sub>3</sub>-CO<sub>2</sub>H: 1.29 mmol). The reaction was stirred for 16 h. A 5.78 mmol amount of 2,3-dichloro-5,6-dicyano-1,4-benzoquinone was added to irreversibly oxidize the monospiroporphyrinogen, and the solution was stirred at air for 60 min. After addition of 1.5 mL of triethylamine, the solvent was removed under vacuum. The free-base porphyrins were a mixture (1/1) of mono- and di-5,15-(spirobifluoren-2-yl)porphyrins, which were separated by chromatography on silica gel using dichloromethane as eluant. The 5-(spirobifluoren-2-yl)porphyrin was eluted first and was separated from the other porphyrin, which was maintained on the top of the column due to polarity. The crude product was crystallized in a mixture of dichloromethane/methanol to afford a red powder of 5-(spirobifluoren-2-yl)porphyrin. Yield: 3%. <sup>1</sup>H NMR (CDCl<sub>3</sub>, ppm): δ –3.63 (NH, s, 2H), 6.91 (H<sub>8</sub>, dd, 1H), 7.15 (H<sub>1'</sub>, dd, 2H), 7.29 (H<sub>7</sub>, td, 1H), 7.30 (H<sub>2'</sub>, td, 2H); 7.36 (H<sub>3'</sub>, td, 2H), 7.53 (H<sub>6</sub>, td, 1H), 7.67 (H<sub>1</sub>, s, 1H), 7.71 (H<sub>4'</sub>, dd, 2H), 8.13 (H<sub>5</sub>, d, 1H), 8.23 (H<sub>4</sub>/H<sub>3</sub>, m, 2H), 8.95 (H<sub>III,VII</sub>, β pyrrole, d, <sup>3</sup>*J* = 4.56 Hz, 2H), 9.30 (H<sub>II,VIII</sub>, β pyrrole, d, <sup>3</sup>*J* = 4.57 Hz, 2H), 9.45 (H<sub>XIII,XVII</sub>/H<sub>XII</sub>, XVIII β pyrrole, 2d, 4H), 10.22 (H<sub>XV</sub> *meso*, s, 1H), 10.26 (H<sub>XX</sub> *meso*, s, 2H). <sup>13</sup>C NMR (CDCl<sub>3</sub>, ppm): 66.8 (C<sub>9</sub>), 104.4 (C<sub>XV</sub> *meso*), 105.4 (C<sub>XX</sub> *meso*), 117.6, 4 (C<sub>4</sub>), 119.5, 119.9 (C<sub>4'</sub>), 120.2 (C<sub>5</sub>), 124.1 (C<sub>1'</sub>), 124.2 (C<sub>8</sub>), 127.8 (C<sub>3'</sub>), 128 (C<sub>2'</sub>), 128.1 (C<sub>7</sub>), 128.2 (C<sub>6</sub>), 130.2 (C<sub>1</sub>), 131.4 (C<sub>XVII,XIII</sub> β pyrrole), 131.2 (C<sub>II,VIII</sub> β pyrrole), 131.25 (C<sub>III,VII</sub> β pyrrole), 131.7 (C<sub>XVIII,XII</sub> β pyrrole), 135.2 (C<sub>3</sub>), 141.3, 141.6, 141.9 (C aromatic rings, spirobifluorene), 145.4 (C<sub>LIX</sub>), 145.45 (C<sub>XI,XIX</sub>), 146.5 (C<sub>IV,VI</sub>), 146.6 (C<sub>XVI,XIV</sub>), 147.8, 148.7, 148.8, 149.6 (C aromatic rings, spirobifluorene). Mass (ESI: 9/1 CH<sub>2</sub>Cl<sub>2</sub>/MeOH) (*m/z*): calcd for C<sub>45</sub>H<sub>29</sub>N<sub>4</sub> (M + H)<sup>+</sup>, 625.23922; found, 625.2398. UV–vis (CH<sub>2</sub>Cl<sub>2</sub>) [*λ*<sub>max</sub>/nm (log *ε*/M<sup>–1</sup> cm<sup>–1</sup>): 230 (4.46), 297 (4.17), 307 (4.20), 402 (5.25), 497 (4.07), 530 (3.38), 570 (3.56), 622 (2.72). CV in CH<sub>2</sub>Cl<sub>2</sub> + 0.2 M Bu<sub>4</sub>NPF<sub>6</sub> (*E*, V vs Fc/Fc<sup>+</sup>): 0.61, 1.06, 1.46.

**(5-(Spirobifluoren-2-yl)porphyrinato)manganese Chloride.** This compound was prepared according to the procedure described for (*meso*-tetrakis(5,10,15,20-spirobifluoren-2-yl)porphyrinato)manganese chloride. The time of reaction is reduced to 5 h. Yield: 82%. <sup>1</sup>H NMR (CDCl<sub>3</sub>, ppm): –23 (m br, β pyrrole, 8H), 50 (m br, H *meso*, 3H). Mass (ESI: 9/1 CH<sub>2</sub>Cl<sub>2</sub>/MeOH) (*m/z*): calcd for C<sub>45</sub>H<sub>26</sub>N<sub>4</sub>Mn (M – Cl)<sup>+</sup>, 677.15379; found, 677.1541. UV–vis (CH<sub>2</sub>Cl<sub>2</sub>) [*λ*<sub>max</sub>/nm (log *ε*/M<sup>–1</sup> cm<sup>–1</sup>): 227 (4.64), 310 (4.1), 365 (4.42), 387 (4.22), 468 (4.63), 562 (3.69), 597 (3.6). CV in CH<sub>2</sub>-Cl<sub>2</sub> + 0.2 M Bu<sub>4</sub>NPF<sub>6</sub> (*E*, V vs Fc/Fc<sup>+</sup>): 0.79, 1.41.

**Catalytic Procedures.** Two different oxidants were used in this work: iodobenzene diacetate; iodosylbenzene. We describe below, for each oxidant, catalytic procedures either for monomers and polymers. Concentrations of alkenes and epoxides were determined by gas chromatography.

**Catalytic Conditions for Monomers.** In a typical experiment, to a 1 mM solution of manganese complex (1 μmol) in dichloromethane (1 mL) was added imidazole (10 μmol), alkene (1000 μmol), and iodosylbenzene (or iodobenzenediacetate) (100 μmol). For PhI(OAc)<sub>2</sub> the solvent was dichloromethane/acetonitrile (7/3) and water (10 μL). In these experiments, the mixture was stirred under an argon atmosphere for 90 min and the alkene epoxidation reaction was monitored by gas chromatography.

**Catalytic Conditions for Polymers.** The contents of (TSP)-MnCl, (DSP)MnCl, and (MSP)MnCl in respective polymers were calculated from the Mn contents in the heterogen catalysts determined by scanning electron microscopy and electronic microanalysis. After the film was scratched out of the electrode, the polymer was crushed to obtain a fine powder. The material was used without any treatment for all catalytic experiments (amount used: poly(TSP)MnCl, 4 mg; poly(DSP)MnCl, 2.4 mg; poly(MSP)-MnCl, 1.6 mg). For a typical experiment with PhIO, imidazole (10 μmol) was added to a suspension of polymer powder in dichloromethane (1 mL) and the reaction was stirred under an argon atmosphere for 15 min. Alkene (1000 μmol) and iodosylbenzene (100 μmol) were then added, and the mixture was stirred for 3 h. The mixture was filtered, and the residue was washed several times with dichloromethane, dimethylformamide, water, and acetone. For a typical experiment with PhI(OAc)<sub>2</sub>, imidazole (10 μmol) was added to the polymer powder in suspension in dichloromethane (1.3 mL) and acetonitrile (0.7 mL), and the reaction was stirred under an argon atmosphere for 15 min. Alkene (1000 μmol), iodobenzene diacetate (100 μmol), and 10 μL of water were then added, and the mixture was stirred for 90 min. The mixture was filtered, and the residue was washed several times with dichloromethane, methanol, and acetone. In all these experiments, the alkene epoxidation reaction was monitored by gas chromatography and the polymer was dried under vacuum and used for another run under the same experimental conditions.

## Results

**Porphyrin and Metalloporphyrin Syntheses.** The series of mono-, di-, and tetraspiroporphyrins have been studied. The synthesis of tetraspirobifluorenylporphyrin, prepared from pyrrole and 9,9'-spirobifluorene-2-carbaldehyde,<sup>63</sup> and dispirobifluorenylporphyrins, prepared from dipyrromethane and 9,9'-spirobifluorene-2-carbaldehyde,<sup>64</sup> have been previously reported.<sup>62</sup> The preparation of *meso*-monospirobifluorenylporphyrin is described herein. The synthetic strategy is adapted from the practical synthesis of *meso*-monosubstituted, β-unsubstituted porphyrins previously reported by Senge et al.<sup>65</sup> Thus, condensation of dipyrromethane, pyrrole-2-carbaldehyde, and 9,9'-spirobifluorene-2-carbaldehyde in the ratio 1:2:1 gave the expected monospirobifluorenylporphyrin but with a low yield (3%).

The manganese (TSP)Mn<sup>III</sup>Cl, (DSP)Mn<sup>III</sup>Cl, and (MSP)-Mn<sup>III</sup>Cl complexes were prepared by treatment of the corresponding free-base porphyrins with MnCl<sub>2</sub> (respectively with 85, 72, and 83% yield), at room temperature, following a method previously reported.<sup>66</sup> <sup>1</sup>H NMR spectra of the complexes show negative shifts for the β-pyrrole-H (~–25 ppm) and positive shifts for the *meso*-H (~+50 ppm) according to expected high-spin Mn(III).<sup>67</sup> This has been confirmed by ClO<sub>4</sub><sup>–</sup> oxidation of these complexes leading to the formation of porphyrin π cation radical Mn(III)

(63) Poriel, C.; Ferrand, Y.; Le Maux, P.; Rault-Berthelot, J.; Simonneaux, G. *Tetrahedron Lett.* **2003**, *44*, 1759–1761.

(64) Poriel, C.; Ferrand, Y.; Le Maux, P.; Simonneaux, G. *Synlett* **2003**, 71–74.

(65) Wiehe, A.; Rypa, C.; Senge, O. M. *Org. Lett.* **2002**, *4*, 3807–3809.

(66) Borovkov, V. V.; Lintuluoto, J. M.; Inoue, Y. *Synlett* **1999**, *1*, 61–62.

(67) La Mar, G. N.; Walker, F. A. *J. Am. Chem. Soc.* **1975**, *97*, 5103–5107.

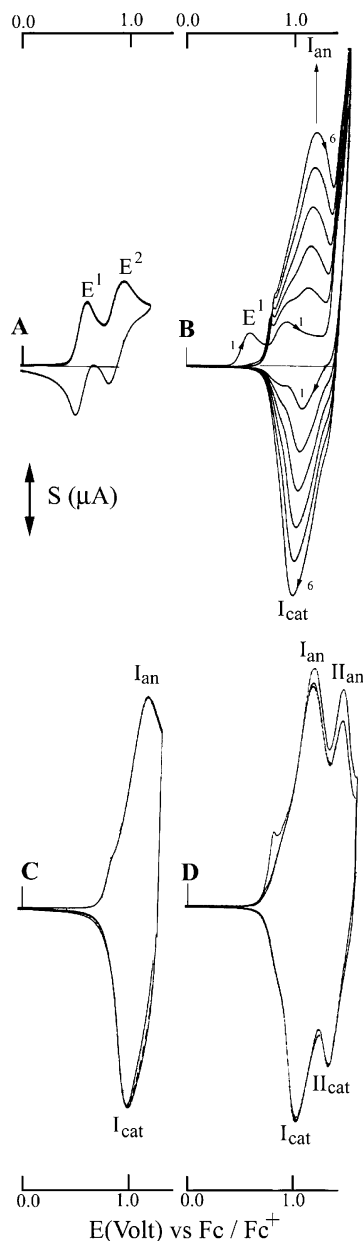


**Figure 1.** Cyclic voltammetry in  $\text{CH}_2\text{Cl}_2$  ( $\text{Bu}_4\text{NPF}_6$ , 0.2 M). Sweep rate:  $100 \text{ mV}\cdot\text{s}^{-1}$ . A, B: in the presence of  $(\text{TSP})\text{H}_2$  ( $2.8 \times 10^{-3} \text{ M}$ ). A: 1 cycle between  $-0.2$  and  $1.15 \text{ V}$ . B: 6 cycles between  $-0.2$  and  $1.45 \text{ V}$ ; working electrode, platinum disk ( $d = 1 \text{ mm}$ ). C: 2 cycles between  $-0.2$  and  $1.25 \text{ V}$ ; working electrode, platinum disk coated by  $\text{poly}((\text{TSP})\text{H}_2)$  prepared in B. D: three cycles between  $-0.2$  and  $1.55 \text{ V}$ ; working electrode, platinum disk coated by  $\text{poly}((\text{TSP})\text{H}_2)$  prepared by potentiostatic oxidation at  $1.5 \text{ V}$  in the presence of  $(\text{TSP})\text{H}_2$  ( $2.8 \times 10^{-3} \text{ M}$ ); amount of charge used for the oxidation,  $2 \times 10^{-4} \text{ C}$ . S:  $4 \mu\text{A}$  in A and  $8 \mu\text{A}$  in B–D.

derivatives. These complexes exhibit the previously reported chemical shifts in  $^1\text{H}$  NMR for  $\beta$  pyrrole hydrogens (approximately  $-35 \text{ ppm}$ ).<sup>68</sup>

**Electropolymerization and Film Formation.** Figure 1A illustrates a typical cyclic voltammogram (CV) of  $(\text{TSP})\text{H}_2$   $2.8 \times 10^{-3} \text{ M}$  in  $\text{CH}_2\text{Cl}_2 + 0.2 \text{ M Bu}_4\text{NPF}_6$  between  $0.0$  and  $1.15 \text{ V}$ . As seen in this figure, two reversible and stable oxidation processes  $E^1$  and  $E^2$  occur with maxima at  $0.6$  and

**Table 1.** Electrochemical Data Obtained in  $\text{CH}_2\text{Cl}_2$  ( $\text{Bu}_4\text{NPF}_6$ ,  $0.2 \text{ M}$ ) at a Sweep Rate of  $100 \text{ mV}\cdot\text{s}^{-1}$  for SBF,  $(\text{MSP})\text{H}_2$ ,  $(\text{TSP})\text{H}_2$ ,  $(\text{MSP})\text{MnCl}$ ,  $(\text{DSP})\text{MnCl}$ , and  $(\text{TSP})\text{MnCl}$ <sup>a</sup>

	$E^1 \text{ (V)}$	$E^2 \text{ (V)}$	$E^3 \text{ (V)}$
SBF			$1.3 + 1.4$
$(\text{MSP})\text{H}_2$	$0.6$	$1.05$	$1.45$
$(\text{TSP})\text{H}_2$	$0.6$	$0.9$	$1.5$ ( $1.4 \text{ sh}$ )
$(\text{MSP})\text{MnCl}$	$0.8$		$1.4$
$(\text{DSP})\text{MnCl}$	$0.7$		$1.3$
$(\text{TSP})\text{MnCl}$	$0.65$	$1.2$	$1.3$

<sup>a</sup>  $E^1$  and  $E^2$  correspond to the oxidation of the porphyrin units and  $E^3$  corresponds to the oxidation of the SBF units as described in Figures 1B and 2B. Potentials referred to ferrocene/ferrocenium.

$0.9 \text{ V}$  versus  $\text{Fc}$ , leading to the  $\pi$ -cation radical and the dication, respectively. Similar voltammograms are observed for  $(\text{MSP})\text{H}_2$ . Due to its insolubility, it was not possible to record voltammograms with  $(\text{DSP})\text{H}_2$ . Potentials of these redox couples are summarized in Table 1 together with  $(\text{TSP})\text{H}_2$  for comparison. Oxidation of free-base tetraphenylporphyrins gave similar results ( $0.5$  and  $0.8 \text{ V}$ ).<sup>69–71</sup>

Oxidation to potential more positive than  $E^2$  leads to a third oxidation wave which maximum  $E^3$  ( $1.45 \text{ V}$ ) is not visible in Figure 1B. However, recurrent sweeps between  $0$  and  $1.45 \text{ V}$  lead to gradual modification of the CVs. At a second sweep, the  $E^1$  wave disappears and a new reversible wave, labeled  $I_{\text{an}}/I_{\text{cat}}$  in Figure 1B, rises between  $0.5$  and  $1.2 \text{ V}$ . Upon cycling, the system  $I_{\text{an}}/I_{\text{cat}}$  grows regularly. After 6 cycles, the platinum is covered by a nonsoluble polymer. No polymer film is formed on successive cycling if the potential sweep does not reach the third oxidation wave. This demonstrates that the formation of the porphyrin  $\pi$ -cation radical or dication is insufficient to induce polymerization of the spirobifluorene groups. The scanning of the potential to oxidation of spirobifluorene ( $>1.3 \text{ V}$ ) causes generation of spirobifluorene radicals, and these radicals in turn initiate polymerization of the oxidized form of  $(\text{TSP})\text{H}_2$ . The rate of polymerization increases when the potential limit is shifted from  $1.3$  to  $1.6 \text{ V}$ . Microcoulometric measurements show that both fluorenyl units are involved in the polymerization reaction (see Supporting Information).

Figure 2A presents the CVs recorded during the anodic oxidation of  $(\text{TSP})\text{MnCl}$  ( $1.3 \times 10^{-3} \text{ M}$ ) and  $\text{Bu}_4\text{NPF}_6$  ( $0.2 \text{ M}$ ) in dichloromethane using a Pt working electrode. The CV recorded between  $-0.2$  and  $1.25 \text{ V}$  (Figure 2A) exhibits the expected well-known two one-electron Mn–porphyrin oxidation<sup>69</sup> at  $E^1 = 0.65 \text{ V}$  and  $E^2 = 1.2 \text{ V}$  (reference  $\text{Fc}/\text{Fc}^+$ ), respectively. No polymerization occurs when cycling in this potential range. These two waves are followed by the irreversible spirobifluorene oxidation wave which maximum  $E^3$  is at  $1.33 \text{ V}$ . The presence of  $\text{MnCl}$  in the porphyrin ring seems to facilitate the oxidation of the spirobifluorene units ( $E^3 = 1.45 \text{ V}$  for  $(\text{TSP})\text{H}_2$ ; vide supra).

When scanning in a potential range including the three waves, the CVs show the appearance and the regular growth

(68) Walker, F. A. In *The Porphyrin Handbook*; Kadish, K. M., Smith, K. M., Guilard, R., Eds.; Academic Press: San Diego, CA, 2000; Vol. 5, pp 81–183.

(69) Kadish, K. M.; Royal, G.; Van Caemelbecke, E.; Gueletti, L. In *The Porphyrin Handbook*; Kadish, K. M., Smith, K. M., Guilard, R., Eds.; Academic Press: San Diego, CA, 2000; Vol. 9, pp 1–219.

(70) Wolberg, A.; Manassen, J. *J. Am. Chem. Soc.* **1970**, *92*, 2982–2991.

(71) Inisan, C.; Saillard, J. Y.; Guilard, R.; Tabard, A.; Le Mest, Y. *New J. Chem.* **1998**, 823–830.

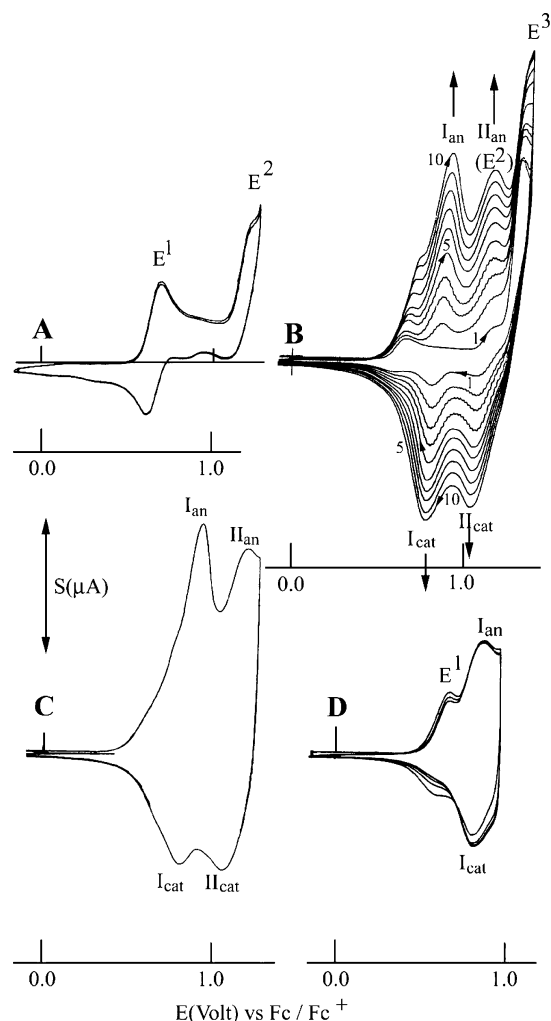


**Figure 2.** Cyclic voltammetry in  $\text{CH}_2\text{Cl}_2$  ( $\text{Bu}_4\text{NPF}_6$ , 0.2 M). Sweep rate:  $100 \text{ mV} \cdot \text{s}^{-1}$ . A, B: in the presence of  $(\text{TSP})\text{MnCl}$  ( $1.3 \times 10^{-3} \text{ M}$ ). A: 2 cycles between  $-0.2$  and  $1.25 \text{ V}$ . B: 10 cycles between  $-0.2$  and  $1.4 \text{ V}$ ; working electrode, platinum disk ( $d = 1 \text{ mm}$ ). C: 1 cycle between  $-0.2$  and  $1.25 \text{ V}$ ; working electrode, platinum disk coated by  $\text{poly}((\text{TSP})\text{MnCl})$  prepared in B. D: three cycles between  $-0.2$  and  $0.95 \text{ V}$ ; working electrode, platinum disk coated by  $\text{poly}((\text{TSP})\text{MnCl})$  prepared by potentiostatic oxidation at  $1.6 \text{ V}$  in the presence of  $(\text{TSP})\text{MnCl}$  ( $1.3 \times 10^{-3} \text{ M}$ ); amount of charge used for the oxidation,  $2 \times 10^{-4} \text{ C}$ . S:  $2 \mu\text{A}$  in A and  $8 \mu\text{A}$  in B–D.

of a new reversible wave centered at  $0.9 \text{ V}$  and the continuous increase in amplitude of  $E^2$  peaks (Figure 2B). The reversibility of the wave centered at  $1.2 \text{ V}$  shows that this wave included both  $E^2$  and the second oxidation wave  $II_{\text{an}}$  of the polyspirobifluorene units. This indicates that a film is formed on the electrode as a consequence of electropolymerization through the spirobifluorene groups (Scheme 1). Table 1 gathers the oxidation potential of  $(\text{TSP})\text{MnCl}$ ,  $(\text{DSP})\text{MnCl}$ , and  $(\text{MSP})\text{MnCl}$ . The three compounds polymerize by anodic oxidation up to the oxidation potential of the spirobifluorene units. Electrodeposition occurs also by oxidation of the fluorenyl units at fixed potential ( $E > 1.30 \text{ V}$ ).

**Characterization of the Polymer Films.** The electrode taken out of the electrochemical cell after oxidation (Figures 1B and 2B), rinsed in dichloromethane, and studied in a new electrolytic solution free of any electroactive species presents

the CV shown in Figure 1C for  $\text{poly}((\text{TSP})\text{H}_2)$  and in Figure 2C for  $\text{poly}((\text{TSP})\text{MnCl})$ , respectively.

For  $\text{poly}((\text{TSP})\text{H}_2)$ , the CV presents a reversible oxidation wave ( $I_{\text{an}}/I_{\text{cat}}$ ), which threshold oxidation potential  $E_{\text{th}}$  is at  $0.7 \text{ V}$ , a value more positive than the first oxidation potential of the porphyrin unit  $E^1$ . This first oxidation process (maximum:  $1.15 \text{ V}$ ) corresponds then to the concomitant oxidation ( $2e^-$ ) of the porphyrin and the first step of the p-doping process of the  $\text{poly}((\text{TSP})\text{H}_2)$ .

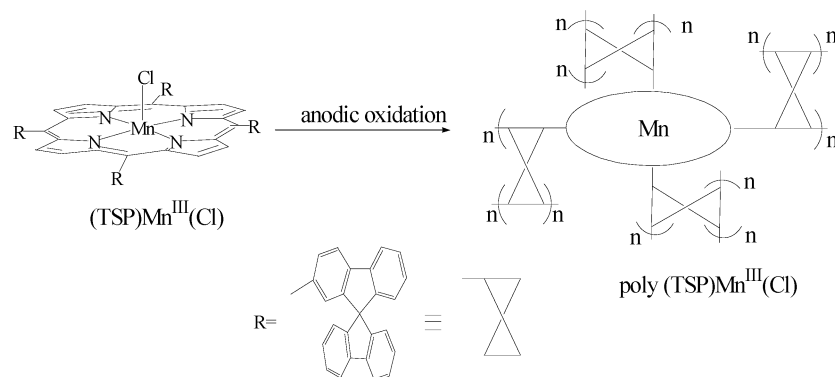
The oxidation of the porphyrin unit is backward at the beginning of the polymer p-doping process. The charge transfer is possible at the beginning of the p-doping process only when the polymer becomes conductor. A study performed up to higher oxidation potential (Figure 1D, in the case of a  $\text{poly}((\text{TSPH}_2))$  obtained along a potentiostatic oxidation) presents a second oxidation wave  $II_{\text{an}}$  with a maximum of intensity at  $1.4 \text{ V}$ . This second wave corresponds to the second oxidation step of the polyspirobifluorene units. The electrochemical response of the  $\text{poly}((\text{TSP})\text{H}_2)$  is stable and reversible between  $0.65$  and  $1.5 \text{ V}$ . This behavior is similar to that of  $\text{poly}((\text{MSP})\text{H}_2)$  (Table 2).

In the case of  $\text{poly}((\text{TSP})\text{MnCl})$ , the CV recorded between  $-0.2$  and  $1.25 \text{ V}$  presents two reversible waves (Figure 2C). The threshold oxidation potential of the polymer is  $\sim 0.5 \text{ V}$ , a value less positive than the oxidation potential ( $E^1$ ) of the manganese porphyrin unit. The first wave which maximum is at  $0.9 \text{ V}$  corresponds to the first oxidation of the porphyrin and to the first step of the  $\text{poly}(\text{SBF})$  p-doping process. The second wave (maximum at  $1.2 \text{ V}$ ) corresponds to the second oxidation step of the metalloporphyrin and to the second oxidation wave of the  $\text{poly}(\text{SBF})$ . Studies performed on a thin deposit of  $\text{poly}((\text{TSP})\text{MnCl})$  (Figure 2D) showed more clearly the difference between  $E^1$  and  $I_{\text{an}}$ . The relative intensities of the two waves may vary with the thickness of the deposits and the potential of the monomer electropolymerization. Finally, the polymer containing manganese porphyrin is stable (no modification of the CVs along recurrent cycles) between  $-0.2$  and  $1.1 \text{ V}$ . The redox potentials of the different polymers are summarized in Table 2. The general behavior of the three different polymers is very similar. The difference is only related to the stability vs oxidation which increases from  $\text{poly}((\text{TSP})\text{MnCl})$ , to  $\text{poly}((\text{MSP})\text{MnCl})$ , and then to  $\text{poly}((\text{DSP})\text{MnCl})$ . The later can be cycled up to  $1.5 \text{ V}$  without significant modification of the CVs.

To study the behavior of  $\text{poly}((\text{MSP})\text{MnCl})$  toward oxidation, spectroelectrochemical experiments were performed. UV–vis spectral changes monitored during anodic oxidation of  $\text{poly}((\text{MSP})\text{MnCl})$  in  $\text{CH}_2\text{Cl}_2 + \text{Bu}_4\text{NPF}_6$  ( $0.2 \text{ M}$ ) are shown in Figure 3. The electronic spectrum of neutral  $\text{poly}((\text{MSP})\text{MnCl})$  obtained as a thin film on an ITO glass electrode shows one series of bands labeled from 1 to 6 related to the neutral manganese porphyrin and one band labeled 7 related to the neutral polyspirobifluorene chain. After progressive oxidation, all bands from 1 to 7 decrease in intensity and a new well-defined band labeled 8 starts to grow at  $500 \text{ nm}$ . The UV–vis spectrum of the final oxidized product shows a broad peak about  $500 \text{ nm}$  and a relatively

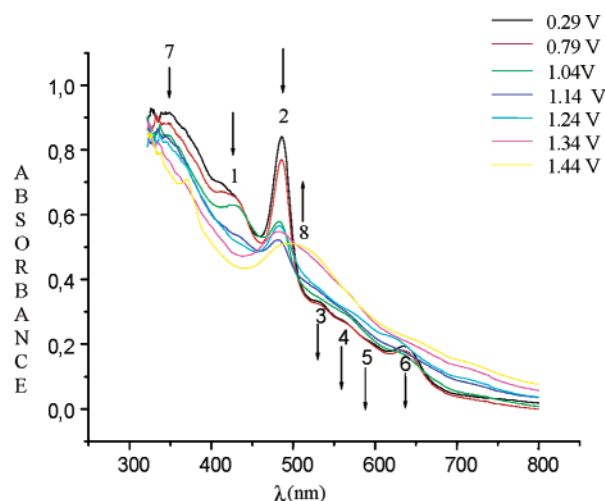


Scheme 1


**Table 2.** Electrochemical Data Obtained in  $\text{CH}_2\text{Cl}_2$  ( $\text{Bu}_4\text{NPF}_6$ , 0.2 M) at a Sweep Rate of  $100 \text{ mV} \cdot \text{s}^{-1}$  for the Different Polymers<sup>a</sup>

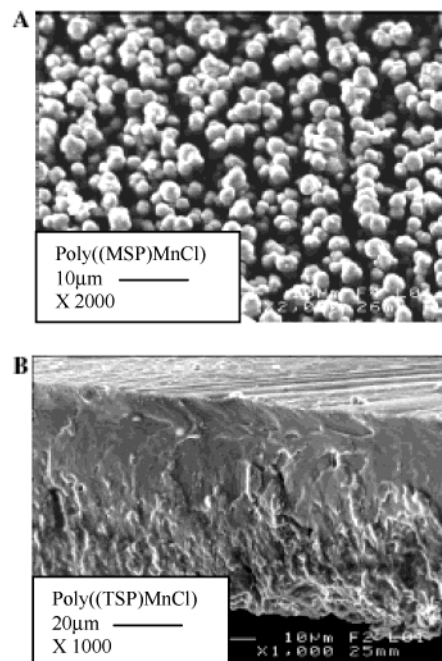
	$(E^1) I_{\text{an}} (\text{V})$	$II_{\text{an}} (\text{V})$	$E_{\text{th}} - E_{\text{lim}} (\text{V})$
poly(SBF)	1.0	1.25	0.5–1.35
poly((MSP)H <sub>2</sub> )	(0.8) 1.05	1.4	0.6–1.5
poly((TSP)H <sub>2</sub> )	1.15	1.4	0.65–1.5
poly((MSP)MnCl)	(0.7) 0.9	1.2	0.5–1.3
poly((DSP)MnCl)	(0.7) 0.95	1.3	0.5–1.5
poly((TSP)MnCl)	(0.6) 0.9	1.2	0.4–1.1

<sup>a</sup>  $I_{\text{an}}$  and  $II_{\text{an}}$  correspond to the two main oxidation waves (see Figures 1C,D and 2C,D).  $E_{\text{th}}$  is the threshold oxidation potential of the polymer, and  $E_{\text{lim}}$  is the higher potential value limiting the stability of the polymer electrochemical response (for  $E > E_{\text{lim}}$ , the oxidation process of the polymer is not reversible). Potentials referred to ferrocene/ferrocenium.


**Figure 3.** Spectroelectrochemical experiments of poly((MSP)Mn(Cl)) recorded from 0.29 to 1.44 V (reference  $\text{Fc}/\text{Fc}^+$ ).

low molar absorptivity compared to the neutral polymer, which is characteristic of a polyspirobifluorene in its p-doped state.<sup>72</sup>

Analysis of the poly((TSP)MnCl) using scanning electron microscopy and electronic microanalysis gives a ratio C/Mn of about 117/1 in agreement with a conserved structure of monomers. To obtain a visual image of the different films, scanning electron micrograph images<sup>73</sup> of poly((MSP)MnCl) and poly((TSP)MnCl) were taken. As shown in Figure 4A, electrochemical polymerization of (MSP)MnCl results in a


**Figure 4.** Scanning electron microscopy of (A) poly((MSP)MnCl) and (B) poly((TSP)MnCl).

structure with 150 nm length and 20–40 nm diameter. Both the density and the size of the nanorods decrease with the increase in the redox cycle. In contrast, Figure 4B shows that electrochemical polymerization of (TSP)MnCl results in a film with very smooth and compact surface presenting a high density. The thickness of the deposits was measured between 50 and 100  $\mu\text{m}$ . All these polymers were conducting materials and scanning electron microscopy experiments were performed without any addition of oxidative reagents.

**Catalytic Oxidation of Alkenes.** We first chose to investigate the catalytic properties of the spiroporphyrin monomers using the epoxidation of a series of alkenes: cyclooctene; styrene; various substituted styrene derivatives. With reactive substrates such as cyclooctene in excess,<sup>74</sup> epoxidation yields were higher than 95% with (TSP)MnCl or (DSP)MnCl, using  $\text{PhI}(\text{OAc})_2$  as oxidant. All the results are summarized in Table 3. The results show that substitution of a *meso* proton by a spirobifluorenyl group changes greatly

(72) Rault-Berthelot, J.; Granger, M. M.; Mattiello, L. *Synth. Met.* **1998**, 97, 211–215.

(73) Hatano, T.; Takeuchi, M.; Ikeda, A.; Shinkai, S. *Org. Lett.* **2003**, 5, 1395–1398.

(74) Battioni, P.; Renaud, J. P.; Bartoli, J. F.; Reina-Artiles, M.; Fort, M.; Mansuy, D. *J. Am. Chem. Soc.* **1988**, 110, 8462–8470.



**Table 3.** Epoxidation of Alkenes by Mn Porphyrin Monomers Using PhIO or PhI(OAc)<sub>2</sub><sup>a</sup>

alkene	yield (%)	epoxide/aldehyde
catalyst, (TSP)Mn <sup>III</sup> (Cl); oxidant, PhIO		
cyclooctene	96	
styrene	75	1.9
4-chlorostyrene	73	4
4-methylstyrene	61	0.7
4-(trifluoromethyl)styrene	65	11.7
3-(trifluoromethyl)styrene	67	4.7
2-(trifluoromethyl)styrene	53	0.9
catalyst, (TSP)Mn <sup>III</sup> (Cl); oxidant, PhI(OAc) <sub>2</sub>		
cyclooctene	95	
styrene	71	1.7
4-chlorostyrene	71	4
4-methylstyrene	73	0.6
4-(trifluoromethyl)styrene	60	6.7
3-(trifluoromethyl)styrene	58	11.2
2-trifluoromethylstyrene	40	0.9
catalyst, (DSP)Mn <sup>III</sup> (Cl); oxidant, PhI(OAc) <sub>2</sub>		
cyclooctene	96	
styrene	95	3.3
4-chlorostyrene	89	12.7
4-methylstyrene	63	0.7
4-(trifluoromethyl)styrene	54	7.8
3-(trifluoromethyl)styrene	41	14.9
2-(trifluoromethyl)styrene	39	6.7

<sup>a</sup> Conditions with PhIO: substrate/oxidant/imidazole/(P)Mn(Cl) = 1000/100/10/1 in 1 mL of CH<sub>2</sub>Cl<sub>2</sub> (catalyst: 1 mM). Conditions with PhI(OAc)<sub>2</sub>: substrate/oxidant/imidazole/(P)Mn(Cl) = 1000/100/10/1 in 1 mL of CH<sub>2</sub>Cl<sub>2</sub>/CH<sub>3</sub>CN (7/3) (catalyst: 1 mM) with 10  $\mu$ L of H<sub>2</sub>O. Yields determined by gas chromatography. Reaction time: 90 min, under Ar.

**Table 4.** Comparative Study of Epoxidation of Cyclooctene by Mn Porphyrin Catalysts Using PhIO or PhI(OAc)<sub>2</sub>

catalyst	oxidant	alkene	yield (%)
poly(TSP)Mn(Cl) <sup>a</sup>	PhIO	cyclooctene	70
poly(TSP)Mn(Cl) <sup>b</sup>	PhI(OAc) <sub>2</sub>	cyclooctene	75
(TSP)Mn(Cl) <sup>c</sup>	PhIO	cyclooctene	96
(TSP)Mn(Cl) <sup>c</sup>	PhI(OAc) <sub>2</sub>	cyclooctene	95

<sup>a</sup> Conditions: cyclooctene/PhIO/imidazole = 1000/100/10 in 1 mL of CH<sub>2</sub>Cl<sub>2</sub> (catalyst: 4 mg) for 180 min. <sup>b</sup> Alkene/PhI(OAc)<sub>2</sub>/imidazole = 1000/100/10 in 1 mL of CH<sub>2</sub>Cl<sub>2</sub>/CH<sub>3</sub>CN (7/3) with 10  $\mu$ L of H<sub>2</sub>O (catalyst: 4 mg) for 90 min. <sup>c</sup> See Table 3. Yields were determined by gas chromatography.

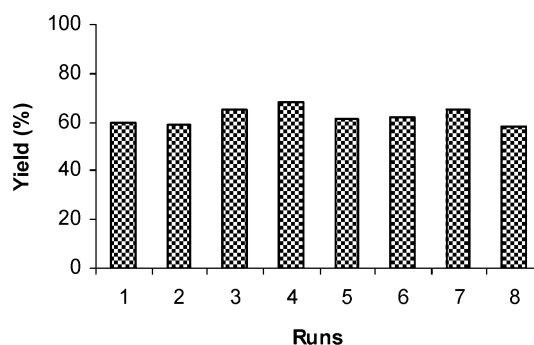
the catalytic efficiency of the manganese porphyrin, at least for the DSP and TSP Mn complexes. Partial degradation of the catalyst was observed when (TSP)MnCl was used in homogeneous reactions. In contrast such a degradation was not observed with the polymers containing Mn porphyrins (vide infra).

Epoxidation reactions using the (spirobifluorenylporphyrinato)manganese polymers were carried out with iodosylbenzene and iodobenzene diacetate as oxygen donors (Table 4). Because it is well-known that the catalytic activity of manganese porphyrins is improved by the use of nitrogen bases as cocatalysts, imidazole was also added in solution.<sup>75,76</sup> The efficiencies and stabilities of the manganese porphyrins as catalysts for epoxidation in free solution and in polymers were examined first using cyclooctene as the substrate. Table 4 shows the epoxide yields from the oxidation catalyzed by the polymers of manganese porphyrins in this study. Mainly, the catalytic activity of the polymer, with PhIO or PhI(OAc)<sub>2</sub>,

**Table 5.** Epoxidation of Alkenes by Mn Porphyrin Polymers Using PhI(OAc)<sub>2</sub><sup>a</sup>

catalyst	oxidant	alkene	yield (%)
poly(TSP)Mn(Cl)	PhI(OAc) <sub>2</sub>	cyclooctene	75
		styrene	65
poly(DSP)Mn(Cl)	PhI(OAc) <sub>2</sub>	cyclooctene	70
		styrene	50
poly(MSP)Mn(Cl)	PhI(OAc) <sub>2</sub>	cyclooctene	95
		styrene	77

<sup>a</sup> Conditions: alkene/PhI(OAc)<sub>2</sub>/imidazole = 1000/100/10 in 1 mL of CH<sub>2</sub>Cl<sub>2</sub>/CH<sub>3</sub>CN (7/3) with 10  $\mu$ L of H<sub>2</sub>O (catalyst: poly(TSP)MnCl, 4 mg; poly(DSP)MnCl, 2.4 mg; poly(MSP)MnCl, 1.6 mg). Yields were determined by gas chromatography; reaction time, 90 min, under Ar.

**Figure 5.** Recyclability of poly(TSP)MnCl for styrene oxidation with PhIO(Ac)<sub>2</sub> as oxidant.

is only slightly inferior to that of the homogeneous system (Table 3). To prove that the catalysis was performed by heterogeneous catalysis and not by the leached manganese porphyrin from the polymer, the supernatant was filtered at the end of the reaction and allowed to react further in the same condition. No additional epoxide was produced indicating that the catalytic activity of the supported porphyrin is truly heterogeneous in nature.

Poly((MSP)MnCl) films obtained from the electropolymerization of monomers containing one spirobifluorene group are probably less cross-linked and hence more permeable than poly((TSP)MnCl) and poly((DSP)MnCl). Table 5 presents a comparative study of the oxidation of cyclooctene (or styrene) with the three polymerized complexes. Activity decreases in the order poly((MSP)MnCl) > poly((TSP)MnCl) > poly((DSP)MnCl).

The recovery and recyclability of the manganese spirobifluorene polymers have been also examined. The catalysts were first tested for activity in the epoxidation of styrene with iodobenzene diacetate leading to 8 recycling steps without loss of activity. The yield for each turn was between 58 and 68% (catalyst: 3 mg) (Figure 5). An overall ~500 catalyst turnovers from eight runs were obtained. If we followed the time course of styrene epoxidation with PhIO, it was also observed that the epoxidation proceeded rapidly in the first run; the yield was 70% after 180 min for styrene oxidation. However, a slow formation of styrene oxide was progressively observed for the other runs. For example, the completion of the reaction took 35 h (yield 52%) for the fifth run. In this case, the total production was equivalent to ~300 catalyst turnovers from five runs.

Furthermore, it is well-known that a large excess of substrate can strongly increase the stability of the catalyst.

(75) Renaud, J. P.; Battioni, P.; Bartoli, J. F.; Mansuy, D. *J. Chem. Soc., Chem. Commun.* **1985**, 888.

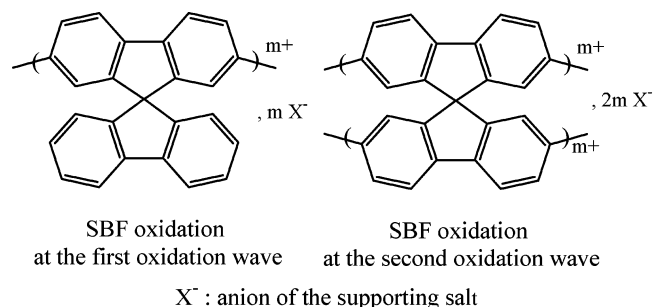
(76) Meunier, B. *Chem. Rev.* **1992**, 92, 1411–1456.

Thus, the activity and stability of the catalyst was also tested in the epoxidation of styrene with a stoichiometric amount of oxidant and olefin (oxidant/olefin/catalyst: 1000/1000/1). Addition of iodobenzene diacetate to alkene leads to 60% of conversion after one run. In this stoichiometric conditions, the manganese polymer was still efficient in alkene epoxidation without any appearance of soluble metalloporphyrins in solution after eight runs. However, a progressive decrease of the yield was observed after the fourth run (yield: 40%). In these conditions, the total production was equivalent to ~1800 catalyst turnovers from four runs.

## Discussion

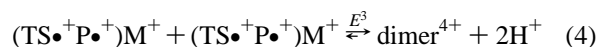
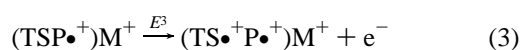
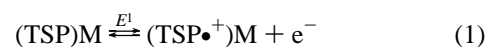
Synthetic manganese porphyrin complexes have been the focus of intense studies as models of the monooxygenase enzyme cytochrome P450, due to their high catalytic activity toward epoxidation and hydroxylation of unactivated C–H bonds.<sup>77,78</sup> Many model systems were divided into two main systems; one contained a soluble manganese porphyrin in homogeneous solution, and the other contained a manganese porphyrin site which was grafted on various insoluble materials or electrochemically fixed on electrodes. In both systems, an active high-valent manganese oxo porphyrin complex was produced as an important intermediate and the amount of the produced oxide increased by the addition of nitrogen base such as imidazole coordinating to the manganese porphyrin. In this paper, we present a new way, using electropolymerization, to produce insoluble polymers bearing manganese porphyrins which can be used as heterogeneous catalysts after being removed from the electrode.

**Electrosynthesis and Characterization.** The formation of conductive and highly stable polyspirobifluorene films on a platinum electrode by the anodic oxidation of spirobifluorene (SBF) in dichloromethane was first reported in 1998.<sup>72</sup> The CVs recorded during SBF oxidation present two irreversible oxidation waves, and it was demonstrated that depending on the oxidation potential, the polymers can present two different structures (see below). Polymerization through the carbon atoms 2 and 7 on each fluorene units was previously demonstrated.<sup>79</sup>



The mechanism (see below) of metalloporphyrin film formation is suggested to be the two electron oxidation of

the metalloporphyrin (eqs 1 and 2) followed by the oxidation of the spirobifluorene units to their radical cations (eq 3), which couple with other radical cations via C2–C7 bonds. Two protons are eliminated at the C2 and C7 carbon atoms forming a dimer containing two metalloporphyrins with two positive charges (eq 4). The fluorene moieties are immediately oxidized at this potential, since the dimer is more easily oxidized than the monomer, leading to a new  $(\text{dimer}^{4+})^+$  radical cation. Thus, the oligomer chain is growing on the electrode surface, yielding a polyspirobifluorenylmetalloporphyrin with the metalloporphyrin in a high oxidation state. It should be noted that the question of metal vs ring oxidation of metalloporphyrins has been the subject of much research because of its relevance to oxidative and electron transfer in heme-containing proteins.<sup>78,80,81</sup> The case of Mn porphyrins is particularly revealing with this respect. With (TPP)MnCl being the first, the Mn(IV) porphyrin radical cation has been characterized.



Thus, modified Pt disk electrodes can be prepared by controlled-potential oxidation at 1.6 V. As expected, the polymerization ability of the different monomers increases with the number of spirobifluorene groups linked to the porphyrin ring. Obviously, it is more difficult to electropolymerize porphyrin bearing only one spirobifluorene group than that bearing four groups. Copolymerization with free spirobifluorene was also possible, but this will not be discussed herein.

Many details of the polymerization reaction remain to be elucidated. One question relates to whether one or both of the two oxidation sites (metal and porphyrin) are maintained after removing the polymer from electrodes. The UV–visible spectrum suggests that these high oxidation states are reduced easily since the Soret band is detected at 468 nm, as observed for the starting manganese monomer (see Supporting Information). If the film was maintained in high oxidation state such as oxomanganese(IV) or oxomanganese(V) porphyrin species,<sup>82</sup> then a decrease in the wavelength of the Soret band would be expected. This is not observed, suggesting that most of the porphyrin units in the film have a manganese in the +III oxidation state. Spectrochemical experiments have also been performed to confirm this hypothesis. Indeed, for both polymers and monomers, the oxidation behavior was very

(77) Cauquis, G.; Cosnier, S.; Deronzier, A.; Galland, B.; Limousin, D.; Moutet, J. C.; Bizot, J.; Deprez, D.; Pulicani, J. P. *J. Electroanal. Chem.* **1993**, 352, 181–195.

(78) Groves, J. T.; Stern, M. K. *J. Am. Chem. Soc.* **1987**, 109, 3812–3814.

(79) Waltman, R. J.; Bargon, J. *J. Electroanal. Chem.* **1985**, 194, 49–62.

(80) Arasasingham, R. D.; Bruce, T. C. *Inorg. Chem.* **1990**, 29, 1422–1427.

(81) Mu, X. H.; Schultz, F. A. *Inorg. Chem.* **1992**, 31, 3351–3357.

(82) Groves, J. T.; Lee, J.; Marla, S. S. *J. Am. Chem. Soc.* **1997**, 119, 6269–6273.

similar. Whether the apparent reduction of the metal atom should be attributed to electron transfer from the solvent or some impurities is uncertain. The same situation is observed with the polymer containing unmetallated porphyrin units, where a Soret band at 429 nm is observed, as expected for a free-base porphyrin.

We do not know what the distribution of chain length is. The fact that current intensity is slightly lower than expected suggests that most of the spirobifluorene units are involved and that the degree of cross-linking is high. It should also be noted that the polymer segments are probably small, due to steric effect, as previously observed with spirobifluorene polymers.<sup>72</sup> However, any dissociation from the rest of the polymer was not observed during catalysis at room temperature.

**Catalysis.** The effectiveness and the resistance to oxidative degradation of the  $\text{Mn}^{\text{III}}\text{Cl}$  porphyrin derivatives bearing spirobifluorene groups as catalysts for the oxidation of styrene and cyclooctene by PhIO with  $\text{Mn}(\text{III})$ -*meso*-tetraspiroporphyrin were first tested in solution for comparison with polymer results. In all reactions, was used a cocatalyst (imidazole) as it has been shown to have a beneficial effect. Styrene epoxide (or cyclooctene epoxide) was found to be the major product in all cases, but aldehydes were also detected as byproducts. The yields obtained are quite good, if we except the results with styrenes bearing electron-withdrawing substituents. These yields are upper than those previously reported for (TFPP) $\text{MnCl}$  and (TPP)- $\text{MnCl}$  but lower than (TDCPP) $\text{MnCl}$ .<sup>83</sup> The deactivation of metal tetraarylporphyrins during oxidation reactions is known to be due mainly to oxidative degradation. When the catalytic centers are fixed in a polymeric matrix, they separated from one another, and this could prevent autocatalytic degradation. Such a good stability of the catalyst is obvious if we consider the recovery and recyclability reported in Figure 5.

**Effect of the Nature of Oxidant PhIO or  $\text{PhI}(\text{OAc})_2$ .**<sup>84,85</sup> Generally,  $\text{PhI}(\text{OAc})_2$  gave a slightly better yields than PhIO, as it has been previously reported in ionic liquids with Mn porphyrins.<sup>86</sup> In our system, the Mn porphyrin catalyst can also be recycled. The two oxidants (PhIO and  $\text{PhI}(\text{OAc})_2$ ) gave good oxidation yields, the small difference may be related to the insolubility of PhIO which leads to a triphasic system. The kinetic profile for  $\text{PhI}(\text{OAc})_2$  is maintained after five reuses. However, it should be noted that the catalytic activity of the polymer decreases after recycling with PhIO. The metalloporphyrin polymer can become deactivated

possibly by precipitation of iodoxybenzene ( $\text{PhIO}_2$ ), obtained from a reaction of disproportionation of iodosylbenzene.<sup>12</sup> Similar behavior was previously reported for the oxidation of alkenes with PhIO using metalloporphyrins supported on cationic ion-exchange resins<sup>35</sup> or covalently bound to silica.<sup>12</sup>

**Effect of Cross-Linking.** Another set of control reactions was performed to investigate the role of cross-linking. Monospiro-, dispiro-, and tetraspirobifluorenyl porphyrins were prepared to investigate the influence of the number of spirobifluorene chains. As expected, the polymerization ability of the different monomers increases with the number of spirobifluorene groups linked to the macrocycle. However, cross-linked polymers prepared from monomers containing two or four spirobifluorene groups present a lower activity than the polymeric films synthesized from the monomer containing only one spirobifluorene moiety. Catalytic activity vs the degree of electropolymerization was previously tested with electropolymerized pyrrole-manganese-porphyrins.<sup>77</sup> In the later case, the decrease of pyrrole units was accompanied by an increase in the amount of the epoxide formed. The better turnover/porphyrin site that we obtained could be due to the presence of only one spirobifluorene group linked to the macrocycle, giving a less dense polymer, as suggested by scanning electron microscopy, in which catalytic centers are more active and more easily accessible to substrate molecules. However, in the absence of direct data concerning film permeability to the substrate, a definitive conclusion is not possible. Furthermore, the reactivity of the catalytically active such as  $\text{Mn}^{\text{V}}=\text{O}$  species<sup>76,78</sup> may be quite different in the three polymers.

## Conclusion

In this work we have shown that stable metalloporphyrin showing good electroactivity over practicable thickness ( $>100$  micron) can be prepared by oxidative electropolymerization of metalloporphyrin complexes bearing spirobifluorene groups. Most of the metalloporphyrin sites are accessible as evidenced by the observed catalytic reaction, after removing the film from the electrode. Thus, polymerization of Mn spirobifluorene porphyrins leads to very efficient catalysts that can be easily recovered and reused. There is no loss of activity after prolonged usage with  $\text{PhI}(\text{OAc})_2$ , which is attributed to protection by the cross-linking of the spirobifluorene chains. We anticipate that the present heterogeneous catalytic system would be potentially applicable to organic synthesis with a special focus on asymmetric catalysis using chiral polymers.

**Supporting Information Available:** Details of electrochemistry and characterization of the polymer film. This material is available free of charge via the Internet at <http://pubs.acs.org>.

IC049641B

(83) Porhiel, E.; Bondon, A.; Leroy, J. *Eur. J. Inorg. Chem.* **2000**, 1097–1105.

(84) Collman, J. P.; Chien, A. S.; Eberspacher, T. A.; Brauman, J. I. *J. Am. Chem. Soc.* **2000**, 122, 11098–11100.

(85) In, J. H.; Park, S. E.; Song, R.; Nam, W. *Inorg. Chim. Acta* **2003**, 343, 373–376.

(86) Li, Z.; Xia, C. G. *Tetrahedron Lett.* **2003**, 44, 2069–2071.